J Electroceram (2008) 21:336–339
DOI 10.1007/s10832-007-9158-7

Phase transition behaviors of $(Na_{1/2}Bi_{1/2})_{1-x}TiPb_xO_3$ thin films

Zhaohui Zhou · Junmin Xue · John Wang

Published online: 26 April 2007

Abstract Ferroelectric thin films of $(Na_{1/2}Bi_{1/2})_{1-x}TiPb_xO_3$ have been synthesized via a sol–gel route. Structural changes of the films were investigated by using X-ray diffraction (XRD) and Raman spectroscopy over the composition range $0<x<0.9$. There occur different nano-sized clusters in the films. More interestingly, in contrast to the previously reported results on $(Na_{1/2}Bi_{1/2})_{1-x}TiPb_xO_3$ bulk ceramics, the ferroelectric thin films exhibit a rhombohedral–tetragonal structure change at $x=0.4$–0.5, together with a long range tetragonal symmetry at $x\geq0.8$. The unique phase transition behaviors are discussed in relation to the growth of $Pb^{2+}TiO_3$ clusters upon the substitution of Pb^{2+} for Na^+/Bi^{3+} cations in the $(Na_{1/2}Bi_{1/2})_{1-x}TiPb_xO_3$ films.

Keywords $(Na_{1/2}Bi_{1/2})_{1-x}TiPb_xO_3$ · Ferroelectric thin films · Phase transitions · Clusters

1 Introduction

Sodium bismuth titanate $Na_{1/2}Bi_{1/2}TiO_3$ (NBT) is one of a handful of perovskite compounds that are derived from substitutions at *A*-sites. Crystal structures, phase transitions and physical properties of NBT, in bulk ceramic forms, have been widely investigated since its discovery by Smolensky in 1960 [1]. The intriguing phase transitions of both NBT and NBT-based solid solutions as a function of composition and temperature make them an excellent model for studies on the phase transition behaviors of relaxor ferroelectrics [2–5]. $(Na_{1/2}Bi_{1/2})_{1-x}Pb_xTiO_3$ [NBPT(x)] is one of such solid solutions that have been reported in the literature. At room temperature, NBT demonstrates a rhombohedral structure with lattice constant of 3.886 Å and a small rhombohedral distortion of 89.6°, while $PbTiO_3$ has a tetragonal symmetry with $c/a=1.066$. As the composition of a phase boundary is largely dependent on the degree of lattice distortion of the solid solution end-members [6], the phase transition in NBPT(x) occurs on the sodium-rich side due to the relatively large lattice distortion of $PbTiO_3$. This has been confirmed by earlier studies on NBPT(x) bulk ceramics [3, 5, 7, 8]. However, there are several large discrepancies concerning the compositions of these phase transitions in the system. For instance, although some investigators proposed the existence of a morphotropic phase boundary (MPB), very differing compositions (i.e., $x=0.1$, 0.13 and 0.13–0.15) have been reported for the MPB [3, 7, 8]. Moreover, Elkechai et al. [5] suggested a biphasic region of $0.1<x<0.18$ in the same system. Although several of these discrepancies have been widely attributed to the microstructure features arising from different synthesis processes, a detailed, systematic study is required, in order to properly understand the nature, compositions and characteristics of these phase transitions.

Further interestingly, most of the previous studies were carried out with NBPT(x) bulk ceramics. The phase transition behaviors of NBPT(x) in thin film forms have not been properly investigated. In this study, we present an investigation into the structural change of NBPT(x) thin films over the composition range $0<x<0.9$, by using X-ray diffraction (XRD) and Raman spectroscopy. Their phase transition behaviors are discussed in relation to the unique microstructure of the films.

Z. Zhou · J. Xue · J. Wang (✉)
Department of Materials Science and Engineering,
Faculty of Engineering, National University of Singapore,
Engineering Drive,
Singapore 119260, Singapore
e-mail: msewangj@nus.edu.sg

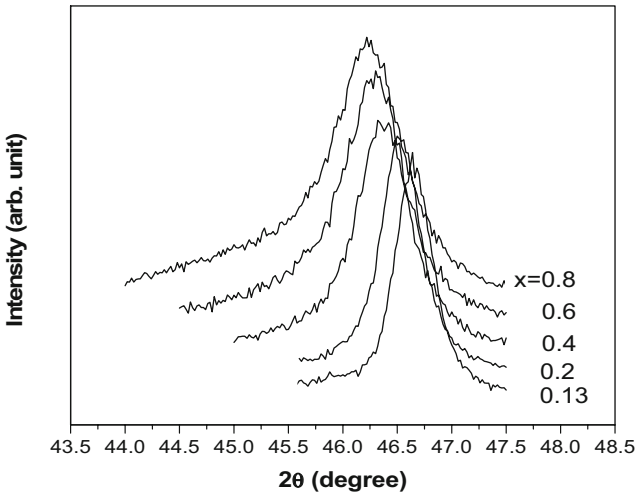

Fig. 1 XRD diffractions of {200} planes for the $(Na_{1/2}Bi_{1/2})_{1-x}Pb_xTiO_3$ thin films with different x values

2 Experiment procedures

The $(Na_{1/2}Bi_{1/2})_{1-x}Pb_xTiO_3$ thin films were synthesized via a multi-step sol–gel route. Starting chemicals included $NaNO_3$, $Bi(CH_3COO)_3$, $Pb(CH_3COO)_2{\cdot}3H_2O$ and $Ti[OCH(CH_3)_2]_4$, which were dissolved into a solvent consisting of ethylene glycol monomethyl ether ($C_3H_8O_2$) and acetic acid at a volume ratio of 5/1.3 to form sol solutions. Concentrations of $(Na_{1/2}Bi_{1/2})_{1-x}Pb_xTiO_3$ in the solutions with different x values were all controlled at 0.4 M. The sol solutions were spin-coated onto Pt/Ti/Si substrate at 3,000 rpm for 30 s. The gel films were then dried at 300 °C for 5 min, followed by thermal annealing at 450 °C for 10 min. Four more layers were deposited and heat treated under the same conditions. The precursor films were then annealed in a rapid thermal processor at 650 °C for 1 min. Compositional analyses by EDAX of the as-annealed films showed that addition of 6 mol % excess lead and bismuth into the compositions gave the most desirable stoichiometry in the $(Na_{1/2}Bi_{1/2})_{1-x}Pb_xTiO_3$ films. Phases in the $(Na_{1/2}Bi_{1/2})_{1-x}Pb_xTiO_3$ thin films were characterized using a X-ray diffractometer (D8 Advanced Diffractometer System, Burker) under detector-scan mode with a fixed incidence angle of 1.5° and a step size of 0.01°. Their phase transition behaviors were further investigated using a Raman spectrometer (Jobin-Yvon Horiba MicroRaman HR800) operated with a cooled GaAs photomultiplier and the 514.5 nm line of an argon green laser as the excitation source.

3 Results and discussion

Lattice distortion and phase transitions in the NBPT(x) thin films were investigated by using X-ray diffraction (XRD). Figure 1 shows the variation of {200} peak as a function of composition. The shift in the low angle peak with the increase in "x" value in NBPT(x) can be explained by the increase of ionic radii ($r_{Pb}{}^{2+}$=1.2 Å, as compared with r_{Na+}= 0.97 Å and r_{Bi3+}=0.96 Å) in association with the substitution of Pb^{2+} for Na^+ and Bi^{3+}. It is known that tetragonal structure demonstrate a splitting in the {200} peak, which was used to identify the existence of MPB in NBPT(x) ceramics in the composition range $0.13<x<0.15$ by Park and Hong [3]. Obviously, no apparent splitting is observed for all compositions in the present study, as shown in Fig. 1. However, a more careful study on the peak profiles showed that two Lorentzian-shape peaks had to be used in order to obtain a best fit of the {200} peaks for the compositions with $x>0.4$, while the peaks for lower x values can be fitted using only one Lorentzian-shape peak (Fig. 2). This indicates that rhombohedral–tetragonal phase transition does occur in the NBPT(x) thin films with the increase of PT level, although the split peaks are overlapped with each other as a result of peak broadening due to small sample thickness. This is

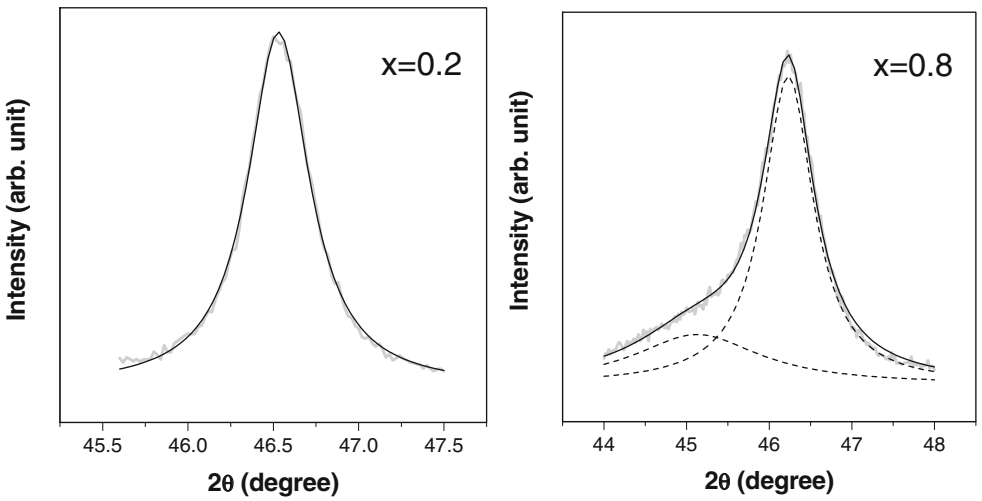

Fig. 2 Deconvolution of {200} reflections in XRD traces for the $(Na_{1/2}Bi_{1/2})_{1-x}Pb_xTiO_3$ thin films. The *gray lines* represent the experimental data, while the *black continuous lines and broken lines* demonstrate the fitting results

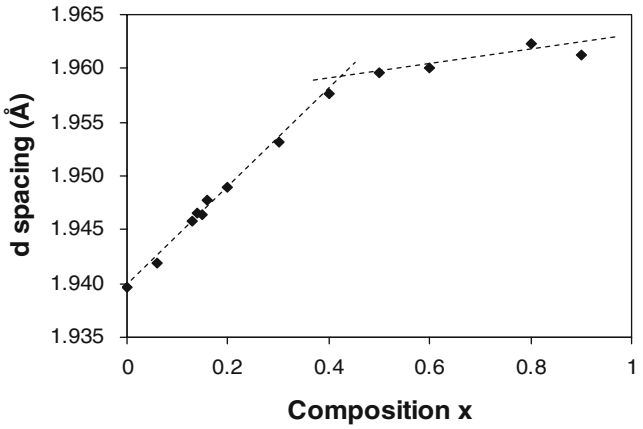

Fig. 3 Dependence of *d* spacing of (200) planes on *x* value in $(Na_{1/2}Bi_{1/2})_{1-x}Pb_xTiO_3$ thin films

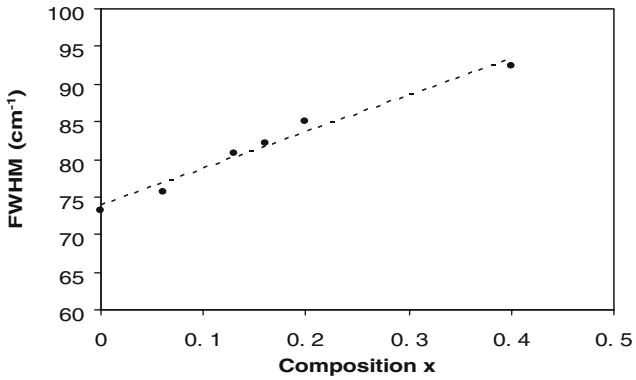

Fig. 5 FWHM of the band at 135 cm^{-1} as a function of *x* value in the $(Na_{1/2}Bi_{1/2})_{1-x}Pb_xTiO_3$ thin films

further affirmed by plotting the d-spacing of (200) plane calculated from the deconvolution of {200} peaks as a function of composition, as shown in Fig. 3, where the slope change observed at $0.4<x<0.5$ gives evidence for a structural change in the films.

Figure 4 shows the Raman spectra for NBPT(*x*) thin films with different compositions as well as the band frequencies as a function of composition derived from spectral deconvolution. Obviously, there is no significant change in the spectra for the compositions of lower *x* values (≤0.4). The band at around 135 cm^{-1} is assigned to A_1 symmetry, which is associated with vibration of cations in A site [9, 10]. More specifically, it has been reported that the presence of this Raman mode implies the existence of local Na^+TiO_3 clusters of several unit cells in NBT [4, 9]. The Raman band corresponding to $Bi^{3+}TiO_3$ clusters was not observed in the present study, while it is expected to locate at very low frequency due to the large Bi mass. According to the "virtual ion" model [11], the 135 cm^{-1} band should shift progressively when Pb substitutes for Na in Na^+TiO_3 clusters, since the "virtual ion" is considered as an ion with the average properties of all cations in the *A*-sites. When force constant change is not taken into consideration, the relationship between the mass and frequency can be described by the following equation:

$$(v_0/v_x)^2 \approx M_x/M_0$$

where v_0 and M_0 are the frequency and mass before substitution, while v_x and M_x are the frequency and mass after substitution. When $x=0.06$, $v_0/v_x \approx (M_x/M_0)^{1/2} = [(0.94*m_{Na}+0.06*m_{Pb})/m_{Na}]^{1/2} = 1.21$. Accordingly, the 135 cm^{-1} band is expected to shift to 111 cm^{-1}, which will be downshifted even further when the bigger ionic size of Pb^{2+} is taken into account. However, no detectable change in the frequency of this Raman band was observed, as shown in Fig. 4. Further interestingly, the 135 cm^{-1} band is getting broadened with the increase in *x* value, as indicated by the increase of the full width of half maximum (FWHM) in Fig. 5. The FWHM of a Raman band is inversely proportional to the lifetime of the corresponding phonon [12], which is in turn closely related to the size of the local Na^+TiO_3 clusters in the case of present study. It is thus believed that the Na^+TiO_3 clusters have to be at least in nanometer size so that the phonon lifetime is long enough to result in a defined Raman peak [9]. As shown in Fig. 4, the intensity of the 135 cm^{-1} band is also weakened with the increase of *x* value. These phenomena can be better explained by the two (or more) mode behavior, where alternative zones (clusters) of nanometer size richer in one constituent than the other are proposed [13]. When Pb substitutes for both Bi and Na, $Pb^{2+}TiO_3$ clusters are formed. As a result, Na^+TiO_3 clusters are reduced in sizes, giving rise to the broadening and weakening of the 135 cm^{-1} band. There is no change in the frequency of this band

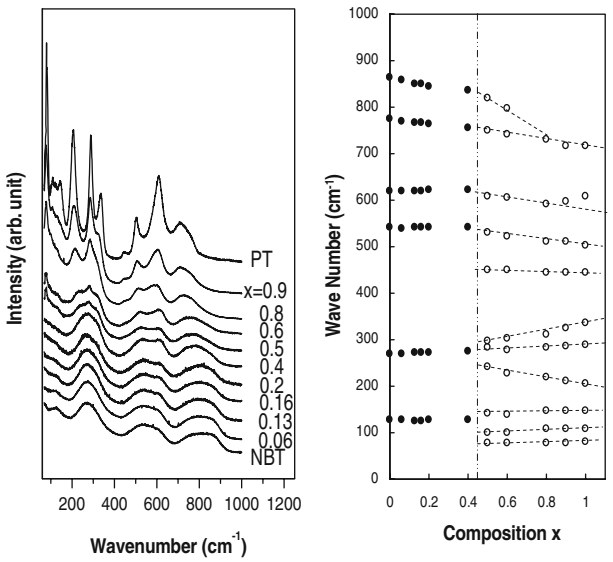

Fig. 4 Raman spectra for the $(Na_{1/2}Bi_{1/2})_{1-x}Pb_xTiO_3$ thin films with different *x* values (*left*) and the band positions as a function of the *x* value (*right*). The *broken lines* in the right figure are guides for the eye to emphasize the change in slope

since both composition and structure remain the same in the $Na^{+}TiO_3$ clusters when x value is low, which is supported by the observations discussed above.

Some drastic changes occur in the Raman spectra when $x>0.4$. Several new bands, located at 78, 109, 146 and 449 cm^{-1}, appear in the spectra. Two of them are underlying bands when $x=0.5$ and 0.6, the introduction of which leads to a better overall fit of the spectra. The band at around 270 cm^{-1} also starts to split into three bands, which shift apart from each other with the further increase in x value. Moreover, bands at 530, 609, 749, 820 cm^{-1} demonstrate a slope change in frequency shift when $x>0.4$. The occurrence of these new bands, observed band splitting, as well as the slope change of frequency shift all indicate a structural change at $x>0.4$, which are well in line with the studies of XRD phase analysis. All bands appear in the spectra at $x>0.4$ can be assigned to the Raman modes for a tetragonal symmetry [14]. $Pb^{2+}TiO_3$ clusters tend to form a stable tetragonal structure but they are constrained by the neighboring $Na^{+}TiO_3$ and $Bi^{3+}TiO_3$ clusters. With the increase in x value and the size of $Pb^{2+}TiO_3$ clusters, such constraining effect become less significant and the phase transition then occur. On the basis of this consideration, it is plausible to conclude that the rhombohedral–tetragonal phase transition observed at around $x=0.4$–0.5 does not occur globally in the films. Instead, some of the $Na^{+}TiO_3$ and $Bi^{3+}TiO_3$ clusters remain in rhombohedral structure. Accordingly, one would further expect a long range ordering of tetragonal symmetry, when x is high enough. This is indeed confirmed by the dramatically enhanced intensity of the Raman bands when the x value is increased further ($x\geq0.8$), as shown in Fig. 4. A strong enhancement in the Raman band intensity suggests the occurrence of a long range ordering of the corresponding phases involved [12, 15, 16]. However, due to the occurrence of the nanometer clusters discussed above, the long range ordering of tetragonal symmetry may not be fully developed in every direction. Nonpolar tetragonal phase with low tetragonality has been observed in rhombohedral NBPT(x) upon heating when x value is low [17, 18]. Therefore, there exist local regions with lower degrees of tetragonality (and thus poorer polarization), due to the compositional inhomogeneity in the NBPT films. Obviously, a detailed study on the domain structure of the NBPT(x) films will be useful for further verification. Indeed, our preliminary studies using piezoelectric force microscope have confirmed the existences of $Pb^{2+}TiO_3$ clusters and local regions with different degrees of polarizability in the NBPT(x) films.

4 Conclusion

Very different phase transition behaviors, as compared to those in their bulk counterparts, have been demonstrated in the ferroelectric thin film of perovskite $(Na_{1/2}Bi_{1/2})_{1-x}TiPb_xO_3$, by using both X-ray diffraction and Raman spectroscopy. The progressive substitution of Pb^{2+} for Na^{+}/Bi^{3+} cations gives rise to the growth of $Pb^{2+}TiO_3$ clusters upon consumption of $Na^{+}TiO_3$ and $Bi^{3+}TiO_3$. The constraining effect among these clusters suppresses the rhombohedral–tetragonal phase transition, which occur locally in the compositions at $x=0.4$–0.5. The $(Na_{1/2}Bi_{1/2})_{1-x}TiPb_xO_3$ in thin film form exhibits a long range tetragonal symmetry when $PbTiO_3$ content (x) is further increased to around 0.8.

Acknowledgment This paper is based upon work supported by the Science and Engineering Research Council—A*Star, Singapore under Grand No 022 107 007. The authors also acknowledge the support of the National University of Singapore.

References

1. G.A. Smolensky, V.A. Isupov, A.I. Agranovskaya, N.N. Krainik, Fiz. Tverd. Tela **2**, 2982 (1960) (Trans. Sov. Phys. Solid State, **2**, 2651 (1961))
2. J.K. Lee, K.S. Hong, C.K. Kim, S.E. Park, J. Appl. Phys. **91**, 4538 (2002)
3. S.E. Park, K.S. Hong, J. Appl. Phys. **79**, 383 (1996)
4. J. Kreisel, A.M. Glazer, P. Bouvier, G. Lucazeau, Phys. Rev., B **63**, 174106-1 (2001)
5. O. Elkechai, P. Marchet, P. Thomas, M. Manier, J.P. Mercurio, J. Mater. Chem. **7**, 91 (1997)
6. B. Jaffe, W.R. Cook, H. Jaffe, *Piezoelectric Ceramics* (Academic, London, UK, 1971)
7. V.A. Isupov, P.L. Strelets, I.A. Serova, Sov. Phys., Solid State **6**, 615 (1964)
8. T. Takenaka, K. Sakata, K. Toda, Ferroelectrics **106**, 375 (1990)
9. J. Kreisel, A.M. Glazer, G. Jones, P.A. Thomas, L. Abello, G. Lucazeau, J. Phys.: Condens. Matter **12**, 3267 (2000)
10. M.S. Zhang, J.F. Scott, Ferroelectr. Lett. **6**, 147 (1986)
11. A.S. Barker, A.J. Sievers, Rev. Mod. Phys. **47**, S1 (1975)
12. J. Kreisel, B. Dkhil, P. Bouvier, J.M. Kiat, Phys. Rev., B **65**, 172101-1 (2002)
13. M.I. Alonso, K. Winer, Phys. Rev., B **39**, 10056 (1989)
14. J.A. Sanjurjo, E. Lopez-Cruz, Phys. Rev., B **28**, 7260 (1983)
15. M.E. Marssi, R. Farhi, X. Dai, A. Morell, D. Viehland, J. Appl. Phys. **80**, 1079 (1996)
16. H. Uwe, K.B. Lyons, H.L. Carter, P.A. Fleury, Phys. Rev., B **33**, 6436 (1986)
17. K.S. Hong, S.E. Park, J. Appl. Phys. **79**, 388 (1996)
18. S.B. Vakhrushev, V.A. Isupov, B.E. Kvyatkovsky, N.M. Okuneva, I.P. Pronin, Ferroelectrics **63**, 153 (1985)